ELSEVIER

Journal of Alloys and Compounds 262–263 (1997) 97–100

Journal of ALLOYS AND COMPOUNDS

Synthesis and characterization of copper intercalated $ZrTe_3$

W. Finckh[a,*], C. Felser[a], W. Tremel[a], G. Ouvrard[b]

[a] *Universität Mainz, Institut für Anorganische und Analytische Chemie, J.-J. Becherweg 24, D-55099 Mainz, Germany*
[b] *Laboratoire de Chimie des Solides, Institut des Matériaux de Nantes, CNRS 2 rue de la Houssinière, F-44072 Nantes Cedex 03, France*

Abstract

Electrochemical copper intercalation in $ZrTe_3$ yields the new metallic ternary phase Cu_xZrTe_3 with a maximum stoichiometry of $x = 1.9$. The charge is balanced by filling the σ^* antibonding Te p bands, as monitored by XANES spectroscopy. The reaction is accompanied by an increase in the a lattice dimension of 9%. This observation is explained by theoretical calculations. © 1997 Elsevier Science S.A.

Keywords: Low-dimensional compounds; Zirconium telluride; Copper-intercalation; XANES spectra; Band structure; Electrical conductivity

1. Introduction

During the past decades, early transition metal chalcogenides have been extensively studied, both because of their physical properties [1,2] and their intercalation chemistry [3]. The two phenomena are intimately related, since the intercalation reaction is driven by a change in oxidation state and therefore accompanied by a change in band filling [4,5]. Electrochemical intercalation therefore can be applied as a tool for controlling the electronic properties of low-dimensional solids [6].

$ZrTe_3$ belongs to a family of trichalcogenides MQ_3 (M = Ti, Zr, Hf, Th; Q = S, Se, Te) [7,8]. The structure (see Fig. 1) contains trigonal MQ_6 prisms condensed via the triangular faces to form infinite chains. One side of the triangle is shortened due to the formation of a Te–Te bond, this leads to a formal oxidation state assignment of $(Zr^{4+})(Te^{2-})(Te_2^{2-})$. These chains are stacked to layers, resulting in an effective eight-coordination of Zr. These layers are mainly held together by van-der-Waals contacts and a very small amount of Te–Te bonding between the partly filled p-orbitals [9].

In contrast to the semiconducting $ZrSe_3$, $ZrTe_3$ is metallic along all directions, shows a resistance anomaly at 63 K [10] and becomes superconducting at 2 K [11]. The origin of the anomaly in $ZrTe_3$ has been the subject of several investigations [10–14]. Band structure calculations [13] predicted a charge density wave (CDW) transition, however, these results became obsolete by a revision of the crystal structure. The occurrence of a CDW in $ZrTe_3$ has been proved by electron diffraction [14]. The structurally related $ZrTe_5$ also exhibits a resistance anomaly, but a CDW seems to be rather unlikely in this case [15].

In order to gain further information about electronic instabilities, we have investigated compounds obtained by controlled chemical variation of the basic structure. Ternary copper transition metal chalcogenides are generally accessible by chemical transport [16], flux growth [17] and intercalation [18]. Whereas Cu_xThTe_3 [19] crystallises in a 'stuffed' $ZrTe_3$ struc-

* Corresponding author.

0925-8388/97/$17.00
PII S0925-8388(97)00336-8

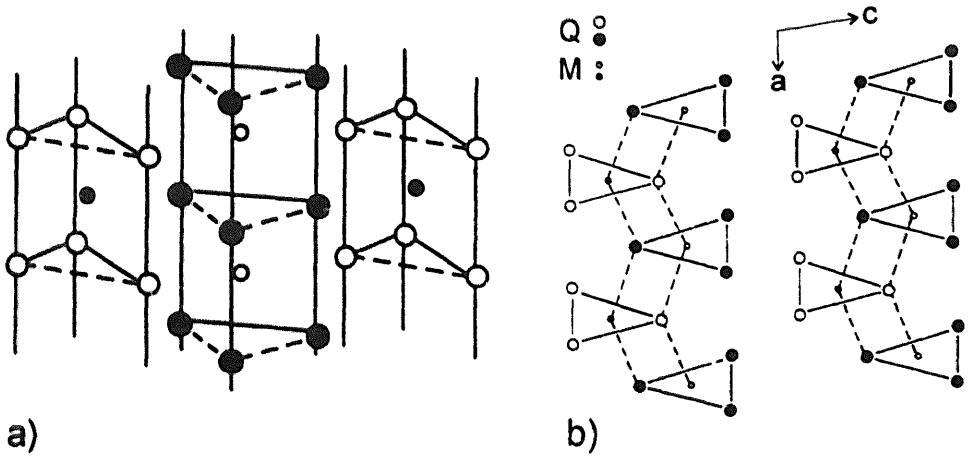

Fig. 1. Crystal structure of $ZrTe_3$: (a) perspective view; (b) projection on the a–c plane.

ture variant with copper in the tetrahedral voids in the van-der-Waals gap, flux synthesis of $Cu_{1.86}ZrTe_3$ [20], Cu_2ThTe_3 [19] and Cu_2ZrTe_3 [17,21] result in more complicated structure types. The mild conditions during intercalation favour the formation of metastable compounds and were therefore most promising for our aim.

2. Experimental

$ZrTe_3$ was synthesised from the elements in the temperature gradient 750 → 650°C with iodine as transporting agent. The crystals were separated manually from oxidic by-products and intimately ground.

For the electrochemical intercalation, $ZrTe_3$ powder (typically 20 mg) was pressed into platinum net (ChemPur, wire 0.06 mm, 1024 meshes cm^{-2}, size 1 cm^2). The electrolyte used was 1 M $CuSO_4$ in 1 M H_2SO_4 and the counter electrode consisted of two copper plates (99.99% +, ChemPur, 1.5 cm^2) coplanar to the probe at a distance of 6 mm. A copper wire (99.99% +, ChemPur, $D = 1$ mm) was used as a reference electrode. A constant current density of 20–100 $\mu A\ cm^{-2}$ was applied and the potential was recorded versus time. The current source (Knick J152) and the Voltmeter (HP 3457 A) were controlled automatically by self-developed software [22].

For the powder conductivity measurements, $Cu_{1.9}ZrTe_3$ was pressed on a square array of four platinum contacts ($D = 2$ mm) and mounted in a helium cryostat. The DC conductivity was measured by standard four probe techniques from room temperature to 5 K and back to room temperature in increments of 2 K.

Powder diffractograms were taken on a D5000 diffractometer (Siemens) in a transmission geometry with Cu $K\alpha_1$ radiation.

The XANES spectra were recorded at the DCI storage ring at LURE (Orsay, France). The storage ring used 1.85 GeV positrons with an intensity of 230 mA. A two-crystal Si(111) monochromator was utilized. For sample preparation, the intimately ground powder was stuck between two layers of adhesive Kapton tape. Te L_I edges were recorded between 4920 eV and 5000 eV in steps of 0.3 eV with an accumulation time of 1 s per point. Energy calibration was performed by comparison with the L_I edge of Te metal, recorded before and after the three samples.

3. Results and discussion

Copper is readily intercalated into $ZrTe_3$ electrochemically. During the reaction, a total of 3.8 electrons per formula unit are transferred. Since Cu is generally incorporated as Cu^I [18], one half of the electrons are consumed for the reduction of Cu^{II}, resulting in a final stoichiometry $Cu_{1.9}ZrTe_3$. Experiments using Cu^ICl/CH_3CN as electrolyte confirm this assumption, as only 1.9 electrons are transferred. Attempts to utilize $AgClO_4/CH_3CN$ to incorporate silver led to a decomposition of the host structure with Ag_2Te as the only detectable product.

The intercalation occurs in two stages: In the first step, 1 $Cu/ZrTe_3$ is included without a considerable change in lattice constants. The second step is accompanied by an increase in the lattice dimension a of approx. 9%. The deintercalation is only partially reversible: 0.5 $Cu/ZrTe_3$ cannot be removed electrochemically. The plateau in potential at 225 mV is interpreted as an oxidative degradation of the host structure. (The potential curve is shown in Fig. 2.) In a second intercalation cycle, Cu enters the host even more readily, as can be seen from the higher potential remaining constant over a large composition range. Presumably, this is due to a high degree of stacking faults being produced during the first cycle. Broad X-ray reflections and the mechanical brittleness of the deintercalated $ZrTe_3$ support this assumption.

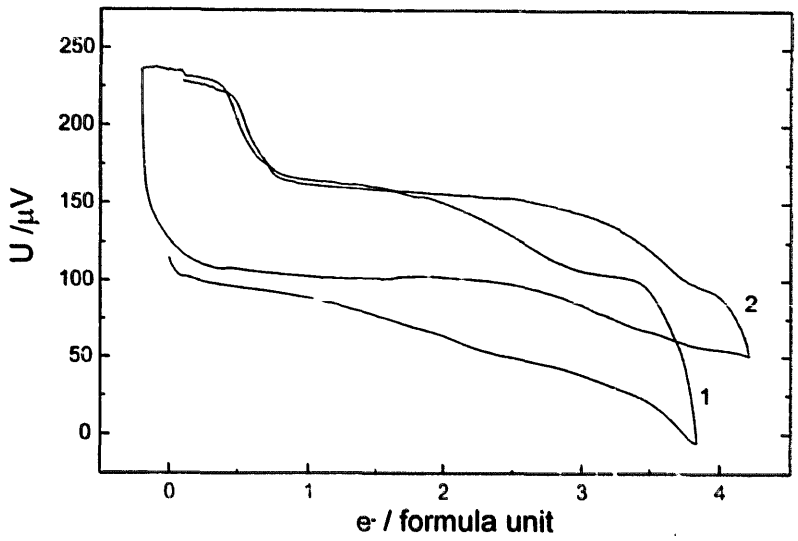

Fig. 2. Electrochemical potential of Cu_xZrTe_3 vs. electron transfer. The reference potential Cu/Cu^{2+} is set to zero.

A comparison of the X-ray absorption near edge structure (XANES) of Cu_xZrTe_3 ($x = 0$, 1, 1.9) on the Te L_I edge (Fig. 3) reveals that the intensity of the white line decreases almost to zero with increasing Cu content. The white line can be assigned to a $2s \rightarrow 5p$ transition [23] and hence probes the amount of empty tellurium p-levels, which are subsequently filled during the reaction [24].

A density of states (DOS) calculation by the LMTO [25] method (Fig. 4) reveals considerable mixing of Zr d- and Te p-levels and hence a partial filling of the Zr d-shell (approx. 1 e^-). Consequently, the Te p-shell is partially emptied, which is compensated by an increase of Te–Te bonding, extending the Te_2 units to one-dimensional Te chains. A detailed analysis of the electronic structure of $ZrTe_3$ results in the conclusion that σ^*-antibonding p-states of the Te-chains dominate at the Fermi level and are responsible for the unusual physical properties [9]. The calculations predict that additional electrons will weaken the Te–Te bonding, causing a repulsive force between the adjacent Te atoms. This view is supported by the XANES results and by the dramatic increase of the corresponding lattice parameter during the reaction.

$Cu_{1.9}ZrTe_3$ shows metallic conductivity (Fig. 5). The small residual resistance ratio $R_{290\,K}/R_{5\,K}$ of approx.

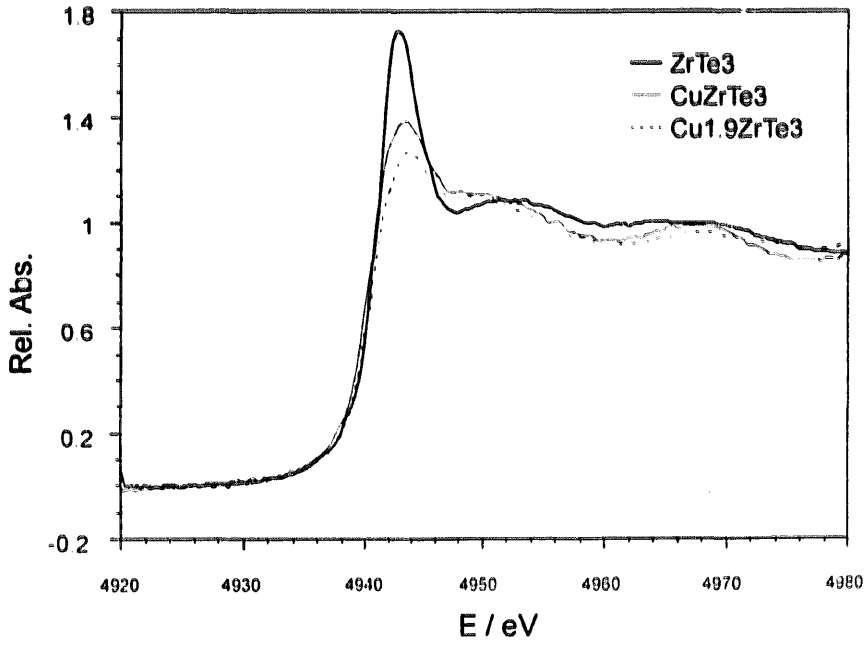

Fig. 3. XANES spectra of the Te L_I edge of $ZrTe_3$, $CuZrTe_3$ and $Cu_{1.9}ZrTe_3$.

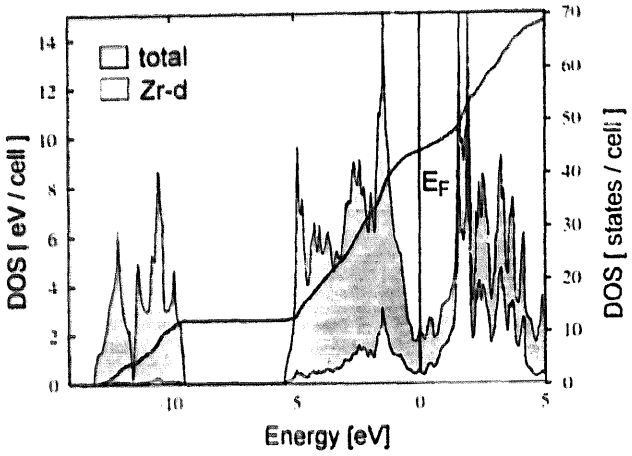

Fig. 4. Total density of states and contributions of Zr *d*-orbitals in $ZrTe_3$.

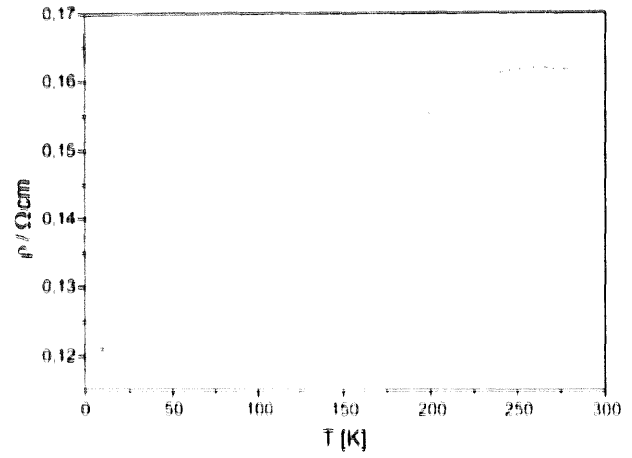

Fig. 5. Powder resistivity of $Cu_{1.9}ZrTe_3$ vs. temperature.

1.25 is due to the large amount of scattering centers both from crystal defects introduced by intercalation and the statistical occupancy of copper in tetrahedral voids. Furthermore, grain boundary effects may contribute to the resistance. Unfortunately, powder investigations cannot reveal changes in the CDW behaviour, since the electron transport mainly follows the chains along which there is highest conductivity but no CDW is observed. Attempts to overcome this obstacle by intercalating single crystals are in progress.

4. Conclusions

$Cu_{1.9}ZrTe_3$ has been prepared by electrochemical intercalation of $ZrTe_3$ and characterised by XANES, X-ray diffraction and resistivity measurements. Both experimental observations and theoretical considerations indicate that σ^* Te–Te antibonding states are filled during the reaction.

Acknowledgements

This research was supported by the Deutsche Forschungsgemeinschaft and the Fonds der Chemischen Industrie.

References

[1] N.P. Ong, J.W. Brill, Phys. Rev. B 18 (1978) 5265.
[2] J. Rouxel (Ed.), Crystal Structures and Properties of Materials with Quasi-One-Dimensional Structures, Reidel, Dordrecht, Netherlands, 1986.
[3] J. Rouxel, R. Brec, Ann. Rev. Mater. Sci. 16 (1986) 137.
[4] R.H. Friend, A.D. Yoffe, Adv. Phys. 36 (1987) 1.
[5] F.W. Boswell, J.C. Bennett, Mater. Res. Bull. 31 (1996) 1083.
[6] G. Giunta, V. Grasso, F. Neri, L. Silipigni, Phys. Rev. B 50 (1994) 8189.
[7] S. Furuseth, L. Brattas, A. Kjekshus, Acta Chim. Scand. A 29 (1975) 623.
[8] S. Furuseth, H. Fjellvag, Acta Chim. Scand. 45 (1991) 694.
[9] C. Felser, W. Finckh, W. Tremel, manuscript in preparation.
[10] S. Takahashi, T. Sambongi, Solid State Commun. 49 (1984) 1031.
[11] H. Nakajima, K. Nomura, T. Sambongi, Physica B 143 (1986) 240.
[12] S.C. Bayliss, W.Y. Liang, J. Phys. C 14 (1981) L803.
[13] E. Canadell, Y. Mathey, M.H. Whangbo, J. Am. Chem. Soc. 110 (1988) 104.
[14] D.J. Eaglesham, J.W. Steeds, J.A. Wilson, J. Phys. C 17 (1984) L697.
[15] G.N. Kamm, D.J. Gillespie, A.C. Ehrlich, T.J. Wieting, Phys. Rev. B 31 (1985) 7617.
[16] W. Tremel, U. Wortmann, T. Vomhof, W. Jeitschko, Chem. Ber. 27 (1994) 15.
[17] P.M. Keane, J.A. Ibers, J. Solid State Chem. 93 (1991) 291.
[18] R. Schöllhorn, in: W. Müller-Warmuth, R. Schöllhorn (Eds.), Progress in Intercalation Research, Kluwer Acad. Publ., Dordrecht, 1994.
[19] W. Tremel, manuscript in preparation.
[20] P.M. Keane, J.A. Ibers, Inorg. Chem. 30 (1991) 3097.
[21] J.F. Mitchell, J.K. Burdett, P.M. Keane, et al., J. Solid State Chem. 99 (1992) 103.
[22] GISELA software package, W. Finckh, Mainz 1996.
[23] J.H. Sinfelt, G.D. Meitzner, Acc. Chem. Res. 26 (1993) 1.
[24] J. Freund, G. Wortmann, W. Paulus, W. Krone, J. Alloys Comp. 187 (1992) 157.
[25] O.K. Andersen, O. Jepsen, Phys. Rev. Lett. 53 (1984) 2571.